

Egyptian Journal of Geology

https://egjg.journals.ekb.eg



Structural setting of the area south of the new administrative capital, Cairo – Suez District, Egypt



Ahmed S. Nagi¹, Waheed Hashem*², Abdelsamad B. Khafagy³ and Adel R. Moustafa²

THE STUDY area is located east of the Greater Cairo region, between the Cairo-Suez Road and L the Cairo-Ain Soukhna Road and is bordered to the northwest by the first phase of the New Administrative Capital City. The main objectives of this study include studying the geological structures of the area and interpreting its deformational history. A geological map on a scale of 1:20, 000 has been constructed showing the exposed Middle Eocene to Oligocene sedimentary rocks with limited basaltic extrusives. These rocks build up the El-Qattamiya and Abu Treifiya Plateaus and the intervening Umm Rihyiat Depression. The Middle and Upper Eocene rocks are dissected by three predominant sets of normal faults, which are oriented in the NNW-SSE, NW-SE and E-W directions. The E-W and some of short NW oriented faults have left-stepped en echelon arrangement that probably originated by dextral wrenching on deep-seated shear zones. The NW and NNW oriented faults are characterized by relatively large lengths and displacements. The E-W oriented en echelon fault belts act as transfer zones that are lying between the major long NW and NNW oriented faults. The tectonic deformation that developed initially these fault sets is assigned herein to pre-date the extrusion of the Oligocene basaltic sheets (i.e. Late Eocene) and were rejuvenated later during the Early Miocene time. The damage zones related to faulting processes show nearly the same rock deformations, whereas the NW-SE and E-W oriented faults have different lengths and throws but exhibit damage zones of equal width. This near constant widths of damage zones could be attributed to the similarity in the deformed carbonate rocks, stress regime, homogenous strain, depth level in Earth's crust, and tectonic events. Two fracture sets are recognized within the fault damage zones, the first (dominant) set is aligned parallel or subparallel to the fault while the second (less dominant) set is aligned oblique to the fault. The first fracture set was developed by the stress regime that formed these faults, whereas the second fracture set was probably developed under the effect of the dextral wrenching that occurred on the E-W oriented deep-seated shear zones.

Keywords: New Administrative Capital, Brittle Deformation, Wrenching Tectonics, Structural Setting, Fault Damage Zones, Cairo-Suez District, Egypt.

1. Introduction

The study area is located east of the Greater Cairo region, south of the first urbanized phase of the New Administrative Capital City and represents the future expansion of the Administrative Capital (Fig. 1). This area is located to the south of the middle part of Cairo-Suez Road which attracted attentions of researches due to its rock-age diversity and intensive tectonic deformation, such as Awad et al. (1953), Shukri (1953), Shukri and Akmal (1953),

Farag and Ismail (1955, 1959), Shukri and Ayouty (1956), Said (1962, 1990), Yousef (1968), Ghobrial (1971), Moustafa et al. (1985), Strougo (1985a, b), Abdel Tawab (1986), Meneisy (1990), Moustafa and Abd-Allah (1991, 1992), Maqbool et al. (2014, 2016), Henaish (2020, 2023), Gamal et al. (2021), Saleh et al. (2021)). Said (1962) and Youssef (1968) reported that the Cairo-Suez District is affected by NW-SE and E-W oriented faults.

*Corresponding author e-mail: whashem71@hotmail.com Received: 02/09/2025; Accepted: 01/10/2025

DOI: 10.21608/EGJG.2025.416376.1126

©2025 National Information and Documentation Center (NIDOC)

¹ WSP for Engineering Consultancy, 13245, Riyadh, KSA

² Geology Department, Faculty of Science, Ain Shams University, 11517, Cairo, Egypt

³ Biological and Geological Sciences Department, Faculty of Education, Ain Shams University, Cairo, Egypt

Abdel Tawab (1986) identified three fault sets that are oriented E-W, NW-SE, and WNW-ESE in the eastern Greater Cairo region and recognized also three E-W elongated belts of en echelon normal faults (Gebel Mokattam, Maadi, and Helwan belts). Moustafa and Abd-Allah (1991) mapped the central part of the Cairo-Suez District and identified the

same three sets of normal faults. They also recognized five E-W elongated belts of en echelon normal faults (Abu Treifiya belt, Wadi Gharba belt, G. El Qattamiya belt, Abu Shama belt, and El Nasuri-El Anqabiya belt) that were developed by the reactivation of E-W elongated deep-seated shear zones lying underneath.



Fig. 1. Satellite image showing the location of the study area relative to the Cairo-Suez District.

Moustafa and Abd-Allah (1992) proposed that the long NW-SE oriented normal found parallel and synchronous genetically with the faults of the Suez rift (Oligo-Miocene age). Whereas the pre-rift E-W fault belts overlie older (Late Triassic in age) deepseated shear zones which utilizing as transfer zones lying between the long NW oriented faults, forming zigzag fault belts in the Cairo-Suez District. Moustafa (2002) confirmed that the E-W en echelon fault belts of the Cairo-Suez District act as transfer zones linking the NW-SE faults in the Cairo-Suez District. Henaish (2023) mapped five types of transfer zones in Gebel Abu Treifiya area, including relay ramps, en echelon step faults, linking folds, breached relay ramps, and transfer faults.

Topographically, the study area contains El-Qattamiya Plateau in the west and Abu Treifiya Plateau in the east which are separated by Umm Rihyiat Depression (**Fig. 1**).

The main objective of this study is to identify the geological structural deformation of the area and its deformation history. In order to achieve these goals, a detailed geological field mapping was carried out on a scale of 1:20,000. The measured data were analyzed to cover the target points.

2. Methodology

The initial office phase of the study involved preliminary photogeological study of the area and literature review. High-resolution satellite imagery from Google Earth, combined with topographic maps on a scale of 1:25,000 served as the base maps for identifying and mapping the key geological features, such as rock unit boundaries and affecting structural features.

The second field phase of the study included a detailed geological mapping and investigation of the fault damage zones. Field mapping involved drawing the outcropped rock units and the structural features. The boundaries of these rock units were mapped in the field on satellite images, and the strike and dip of these rocks were measured, in addition to the fault-slip and damage zone data. Also, fault traces were mapped in the field, and the strike and dip of the faults were measured wherever possible. The damage zones of some faults were studied using scanline surveys. These surveys involved measuring the orientation and distribution of fractures on both sides of the fault zones along a 30m long scan line on one or both sides of the studied faults.

The final phase of study was completed in the office, where all field data were compiled, analyzed, and interpreted. The obtained information

was transferred onto topographic base maps, and a detailed geological map was produced. This map was supplemented with constructing of geological cross-sections to illustrate the subsurface continuation of the different rock units and their dissecting structures. Additionally, the scanline survey data were analyzed to evaluate the extent and characteristics of fault damage zones.

3. Stratigraphy

The geological map of the Greater Cairo area (Egyptian Geological Survey and Mining Authority, 1983) classified the exposed Eocene rock units of this area into two facies: Cairo facies and Helwan facies. Strougo (1985 a, b) compiled the terminology of the rock units of the Greater Cairo area and identified their lithologic and paleontological characteristics. Strougo and Abd-Allah (1990) studied the lateral continuity of these stratigraphic units in the Greater Cairo and extended the use of these formal units over the north-central part of the Eastern Desert.

The exposed sedimentary rocks in the study area range in age from the Middle Eocene to the Oligocene (**Fig. 2**). These sedimentary rocks are intruded by basaltic rocks in a few locations and are partially covered by Quaternary deposits in some places. Three Middle Eocene rock units exist in the area, which are the Observatory, El-Qurn, and Wadi Garawi Formations (from older to younger). The Upper Eocene rocks belong to the Wadi Hof Formation that occupies mainly low structural and topographic areas. In addition, there are limited exposures of the Oligocene Gebel Ahmar Formation. A brief description of the mapped rock units is provided below.

3.1 Observatory Formation

The Observatory Formation represents the oldest exposed rock unit in the study area and has a wide exposure. It forms large scarps and most of the well-known topographic heights in the area. This rock unit is composed mainly of white chalky limestone, with a characteristic nodular limestone bed in the middle (**Fig. 2**). This formation is further distinguished by very thin bands of chert concretions, which characterize its lower part (**Fig. 3**). The largest thickness of the Observatory Formation is measured at Abu Treifiya Plateau, where the formation is about 65m thick.

3.2 El-Ourn Formation

El-Qurn Formation has the widest exposures in the study area, whereas its rock sequence is capping

most top surface of the existing plateaus. It conformably overlies the Observatory Formation, with a clearly identified contact marked by a yellow-colored bench. The lower part of El-Qurn Formation is composed of highly fossiliferous, argillaceous to marly limestone that is overlain by white limestone. Whereas its upper part comprises thick, flaky, less fossiliferous limestone, which is observed only at Abu Treifiya Plateau in the eastern side of the study area.

Age	Formation	Lithology	Description	Thickness (m)	
			Basalt flows		
Oligocene	G. Ahmar Formation		Variegated sands and gravels with quartizite and some chert bands at the top	~ 30	
Late Eocene	Wadi Hof Formation		Intercalated sandy limestone and marl with <i>Carolia, Plicatula,</i> and <i>Anisaster sp.</i>	> 35	
Middle Eocene	Wadi Garawi Formation		Intercalated yellow sandstone and green shale	~ 16	
	El Qurn Formation		Intercalated limestone and marl with <i>Nummulites, Oysters</i> , and <i>Plicatula sp.</i> In addition to some non-fossiliferous flaky limestone at the top Yellow argillaceous limestone	~ 45	
	Observatory Formation		White chalky limestone with Echinoides, Nummulites, Vulsella, and Huyella sp. Dolomitic limestone ledges	~ 65	
			White chalky limestone		

Fig. 2. Composite stratigraphic section showing the exposed rock units in the study area (modified after Abd-Allah, 1988).



Fig. 3. Field photograph showing bands of chert concretions (marked by arrows) in the lower part of the Observatory Formation.

3.3 Wadi Garawi Formation

The Wadi Garawi Formation represents the uppermost Middle Eocene rock unit and is exposed in the topographic lows within the western side of the area. This formation consists of sandy marl,

light green marl, and shale which are interbedded by cross-laminated sandstone layers.

3.4 Wadi Hof Formation

The Wadi Hof Formation is the youngest exposed Eocene rock unit in the study area. The lower contact of the Wadi Hof Formation is not detected in the study area, but it is assumed to conformably overlie the Wadi Garawi Formation. The Wadi Hof Formation is exposed in the structurally low downfaulted areas and consists of sandstone, sandy limestone, and marl (from base to top). The Wadi Hof Formation is distinguished by the presence of several fossiliferous banks rich in small size *Carolia placunoides* (**Fig. 4**).



Fig. 4. Field photograph showing a bank of *Carolia placunoides* within Wadi Hof Formation. (Scale is 15 cm long).

3.5 Gebel Ahmar Formation

The Upper Eocene rocks of the Cairo-Suez area are unconformably overlain by the Oligocene clastics of Gebel Ahmar Formation (Said, 1962). The Gebel Ahmar Formation is exposed in a number of grabens in the western and northern parts of the study area. The Oligocene rocks are composed of varicolored, unstratified sands and gravels, with occasional occurrences of sedimentary quartzites and fragments of silicified wood of various sizes (**Fig. 5**). This formation was affected by rising silica- and iron-bearing solutions, which form local topographic heights near some of the fissures (Shukri and Akmal, 1953).

3.6 Basalt Flows

Basaltic flows unconformably wrap the Oligocene sands and gravels of the Gebel Ahmar Formation in the study area and its vicinity. Basalt exposures are located within a NW-SE elongated graben in the western part of the study area (**Fig. 6**).

4. Structures

Detailed field mapping of the study area revealed the presence of 62 normal faults, in addition to 35 structural lineaments (**Fig. 7**). These lineaments were detected on satellite imagery and some of them may represent inferred faults. Slickenside lineations on the fault planes confirm that most of the mapped faults witnessed normal dip-slip displacement. However, there are two faults that show strike-slip component, with a sinistral sense of slip. The arrangement and pattern of the normal faults in the study area resulted in the formation of prominent structural styles, such as horsts, grabens, and relay ramps (**Fig. 8**).



Fig. 5. Field photograph showing the varicolored, unstratified sands and gravels of Gebel Ahmar Formation in the study area.



Fig. 6. Field photograph showing basalt flows within the Oligocene sands and gravels in the area.

The mapped faults can be divided into three predominant fault sets, according to their orientation. These are NNW-SSE, NW-SE, and E-W oriented fault sets (**Fig. 9**). The description of each fault set is given below.

4.1 NNW-SSE oriented fault set

The NNW-SSE oriented fault set involves 20 faults, which represent about 32% of the mapped faults. These faults are oriented between N330° and N360° and have normal dip-slip displacement and the dip

angles of their planes range between 60° and 70°. The displacements of these faults indicate that 9 faults have displacements less than 50 m, and the remaining faults have displacements ranging

between 50 and 120 m (**Fig. 10**). Two of these faults have trace lengths greater than 5 km, 13 faults have lengths ranging from 1 to 5 km, and each of the remaining faults has length less than 1 km.

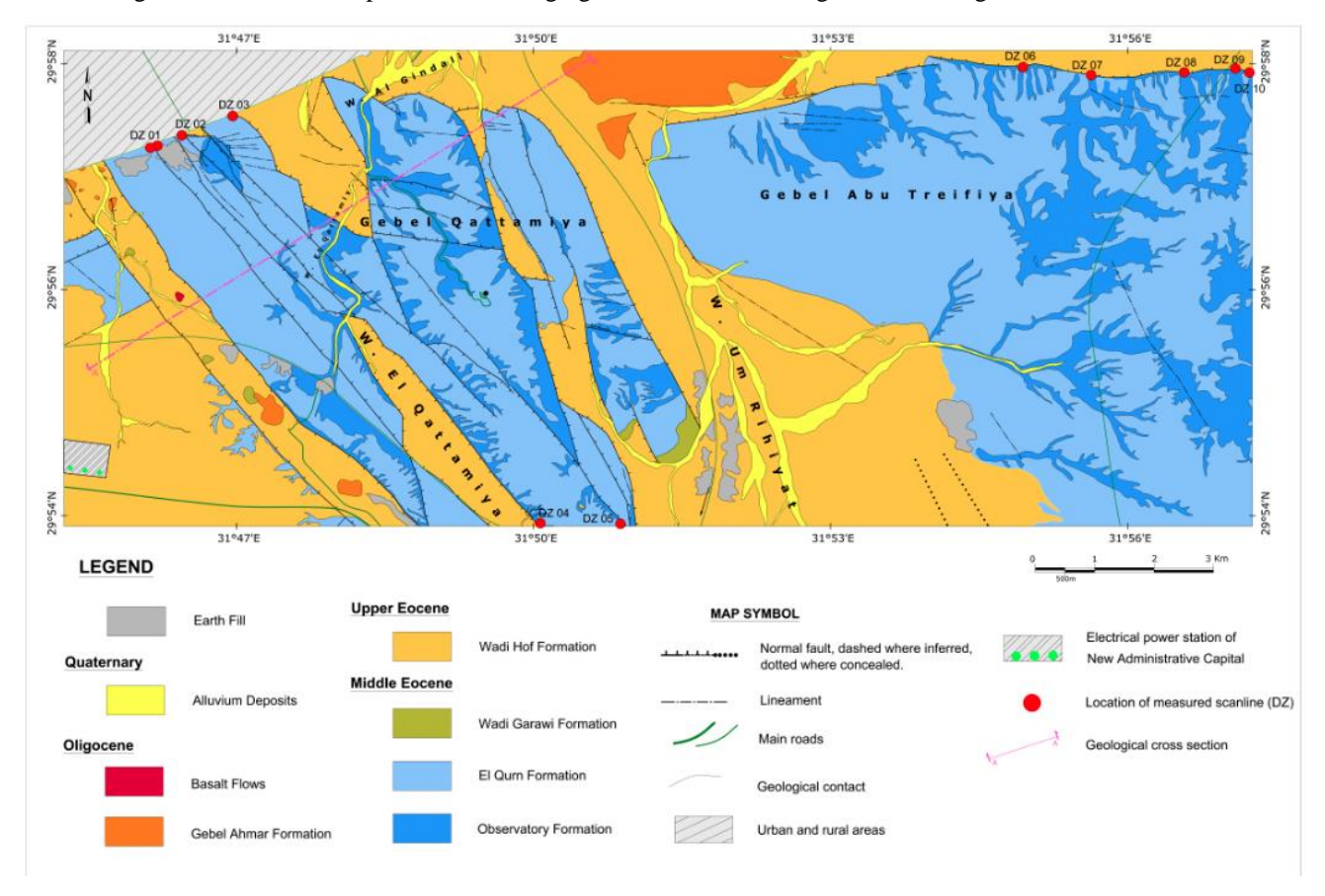


Fig. 7. Simplified geological map of the study area.

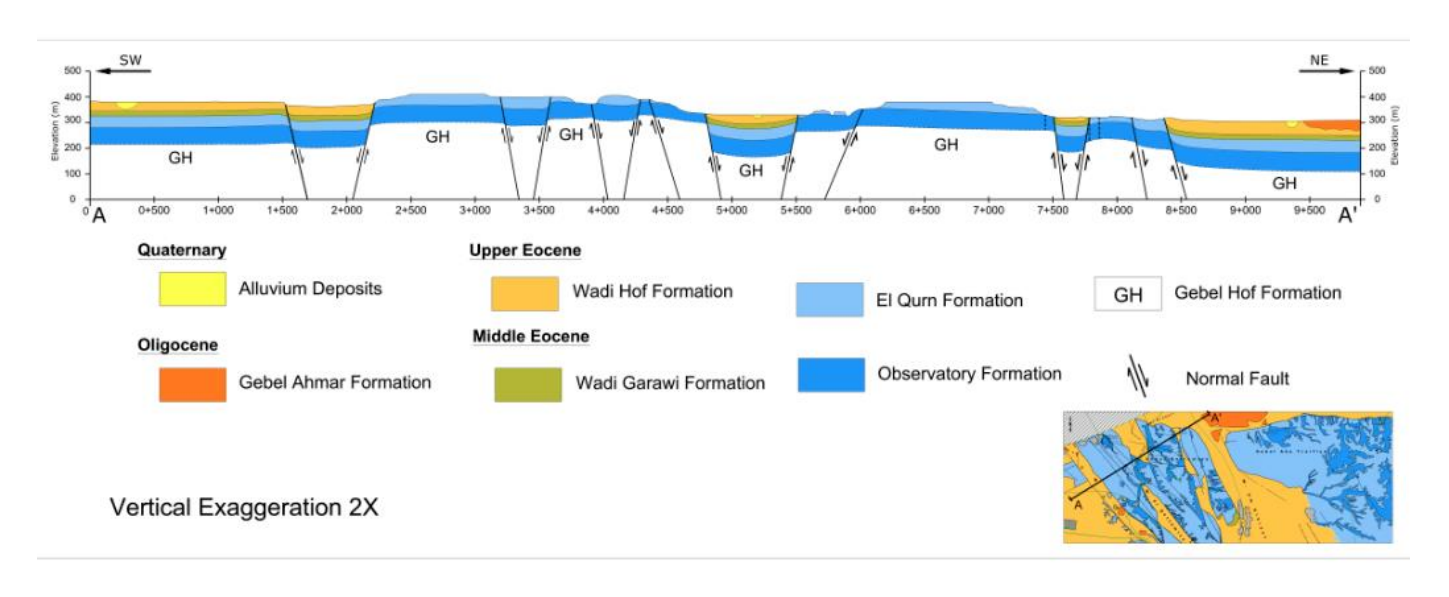


Fig. 8. Structural cross section A-A showing horsts and grabens in the area. See Figure 7 for location.

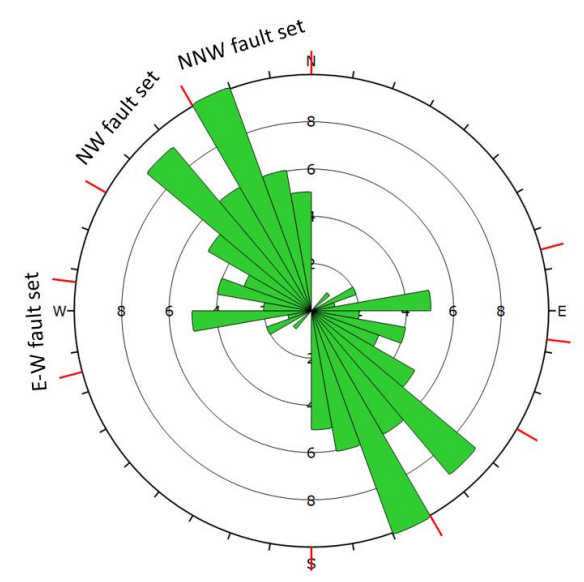


Fig. 9. Rose diagram showing the orientations of mapped faults of the study area (total number = 62 faults).

4.2 NW-SE oriented fault set

The faults of this set involve 22 faults that represent approximately 35% of the mapped faults of the area. The orientations of these faults range between N300° and N330° and have normal dip-slip displacement with dip angles ranging from 60° to 80°. Only one fault of this set displays diagonal-slip displacement, with a normal dip-slip component and a sinistral strike-slip component. The fault displacements of this set indicate that 9 faults have displacements less than 50 m, and the remaining faults have displacements ranging from 50 to 105m (**Fig. 10**). The trace lengths of most of these faults are less than 5 km, and only 4 faults have lengths greater than 5 km.

Many of the NW and NNW oriented faults form the borders of the high plateaus in the study area, including the western side of El-Qattamiya Plateau and the eastern and western sides of Gebel Abu Treifiya. These faults also form the NW to NNW oriented grabens, where the main wadis; such as Wadi El-Qattamiya and Wadi Umm Rihiyat.

4.3 E-W oriented fault set

Eleven faults belong to this fault set and are oriented between N259° and 277°E (**Fig. 9**). They represent about 18% of the mapped faults. These faults display normal dip-slip displacement, and their dip angles range from 62° to 80°. Based on the field measurements, these faults exhibit relatively moderate displacements ranging from 15 to 65m, except for only one fault that displays a larger

displacement approaching about 90m (**Fig. 10**). Most of the faults of this set have lengths less than 2 km. The E-W oriented faults bound the northern side of El-Qattamiya Plateau and the northwestern escarpment of Abu Treifiya Plateau. These faults form relatively small horsts and grabens in the study area.

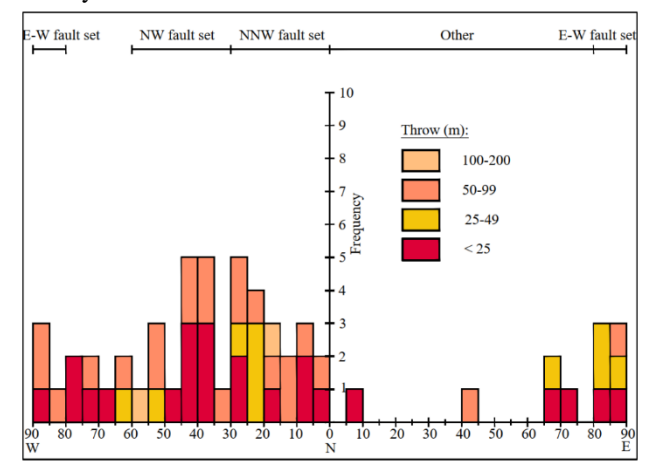


Fig. 10. Orientation-frequency histogram for the 62 mapped faults showing their displacement values.

Some of the E-W- and NW-trending faults have en echelon arrangement within two elongated belts, such as Abu Treifiya Belt and Maadi-Gebel El-Qattamiya Belt. Within each belt, the en echelon faults have left-stepping arrangement. The Abu Treifiya en echelon fault belt, located in the northeastern part of the study area (**Fig. 7**). This belt consists of several left-stepping en echelon faults. Relay ramps are observed and mapped between the ends of some of these faults. A relay ramp is defined as an area of local dip increased where en echelon-arranged to normal faults step each other (Moustafa et al., 1985).

A total of 35 structural lineaments were detected in the study area, representing approximately 36% of the total mapped structures of the area. These lineaments were identified and detected on satellite imagery. They have closely the same orientations as those of the mapped faults, where they exist in three main sets trending also in NNW–SSE, NW–SE, and E–W. In addition to these, 9 faults exhibit random orientations different from these mentioned sets.

It is worth mentioning that the western part of the study area, including Gebel Qattamiya, is characterized by more faulting density, when compared by the eastern part of the area, including Gebel Abu Treifiya. This differences in the density of faulting could be related to (i) strain shadow if

the thickness and mechanical homogeneity of the sedimentary cover are the same between the two areas and (ii) the presence of more Precambrian deep-seated faults affecting the area of the highdensity faulting.

5. Fault Damage Zones

The scanline survey method was conducted to investigate the damage zones in the study area. The analysis of the measured fractures within the fault damage zones revealed consistent characteristics across most of the studied scanlines. Based on these observations, the whole fault damage zone can be further subdivided into three distinct zones, including the background fracture density. The background fracture density is determined by measuring fracture spacing at predetermined locations away from faults.

The innermost part of the fault damage zone (close to the fault) is marked by extremely deformed rocks, often appearing as brecciated material or gouge. This area contains multiple slip surfaces, with very tight fractures having little to no filling material. Moving outward, the next area of the damage zone displays intensive, closely spaced fracturing, with narrow apertures typically filled with fine-grained clastic sediments. Further away, the fracture spacing increases, and the apertures become slightly opened, with silty to sandy clastic infilling and iron oxide staining.

The damage zones of six different faults were measured. The primary criterion for selecting the locations of the scanlines was the suitability of the exposed sections either within the footwall, hanging wall, or both blocks of the concerned faults. Ten damage zones distributed at six different faults were measured, and the results are shown in **Table 1**.

The (DZ 09) location is situated across an E-W trending fault and is discussed in detail as an example and illustrated in Fig. 11. At this location, perpendicular scanline measurements conducted on both the hanging wall and footwall blocks (Figs. 11 and 12). The scanline extended to about 24m on the footwall and 30m on the hanging wall, totaling 54m in length on both sides of the main fault (trending N 100° and dips 80° in NNE direction) (Fig. 13). A total of 60 fractures were recorded in the footwall, while 57 fractures were measured in the hanging wall. Fracture orientation analysis revealed one dominant fracture set in the footwall, trending subparallel to the fault (N 100° to N 110°). The hanging wall exhibits two fracture sets: dominant set aligned subparallel to the fault (N 100° to N 110°), and a less dominant set is trending in E-W (Fig. 13).

The fracture characteristics vary significantly across the scanline in each of the three portions of damage Zone DZ 09 (named here Zones 1, Zone 2, and Zone 3), as described below and as shown in **Fig. 14**:

Zone 1 (0 - 4 m): This zone is located adjacent to the fault plane (or trace), exhibiting a high density of fractures. The rock mass in this zone is highly weathered due to intense deformation. The fractures in this zone are predominantly parallel to the fault plane and have tightly closed apertures.

Zone 2 (4 - 19 m): In this zone, the fractures are both parallel and conjugate relative to the fault plane. The apertures are small to tight.

Zone 3 (19 m to end of the damage zone): Moving further from the fault plane, the fracture spacing increases and most of the fractures in this zone are oriented parallel to the fault plane, whereas the apertures become relatively wider.

Table 1.	Data of th	ne measured	fault	damage	zones in	the study	area. S	ee figure 7	for loca	ition.

Damage Zone (DZ) Number		Fault Orientation	Fault throw	Fault length	Wall block	Damage zone
			(m)	(Km)		half width (m)
DZ 01		320°/65°NE	59	8.6	Footwall	21
					Hanging Wall	22
DZ 02		320°/65°NE	5	4.3	Footwall	24
DZ 03		323°/71°NE	65	1.3	Footwall	26
DZ 04		301°/60°SW	105	4.5	Footwall	21
DZ 05		316°/70°NE	55	1.3	Footwall	32
Fault (F-60)	DZ 06	106°/72° NE		5.5	Footwall	20
					Hanging Wall	19
	DZ 07	100°/72° NE			Footwall	20
	DZ 08	108°/70° NE	63		Footwall	18
	DZ 09	100°/80° NW			Footwall	19
					Hanging Wall	19
	DZ 10	113°/80° NE			Footwall	25



Fig. 11. Field photograph showing a location for scanning the damage zone of DZ 09 fault blocks. See figure 7 for location.

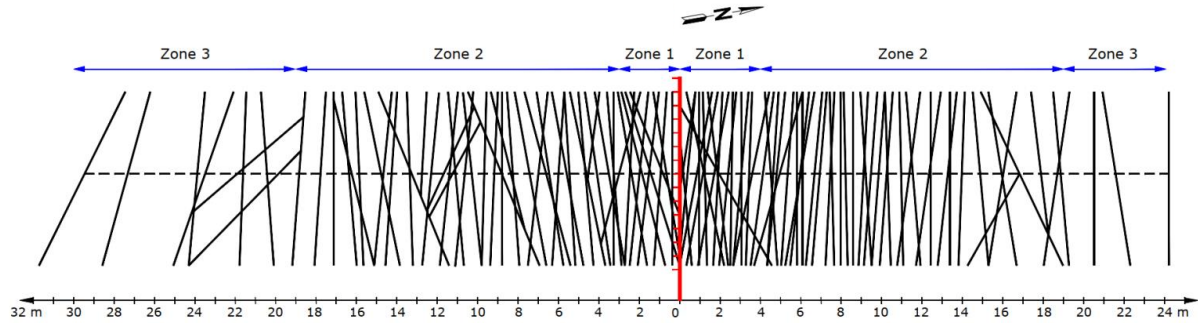


Fig. 12. Representation of the scanline fracture orientations in each zone with respect to the trend of the fault (N100°/80°NNE, red line) at DZ 09. See figure 7 for location.

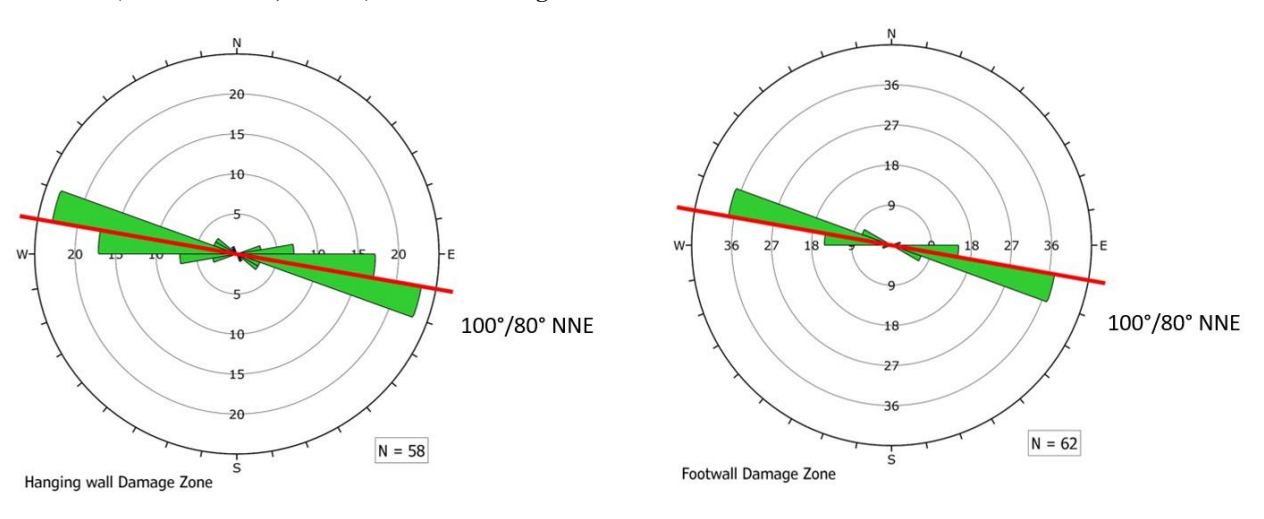


Fig. 13. Rose diagrams of the measured fractures along the scanline of DZ 09 (Fig. 12). Red line represents the orientation of the fault ($N100^{\circ}/80^{\circ}NNE$).

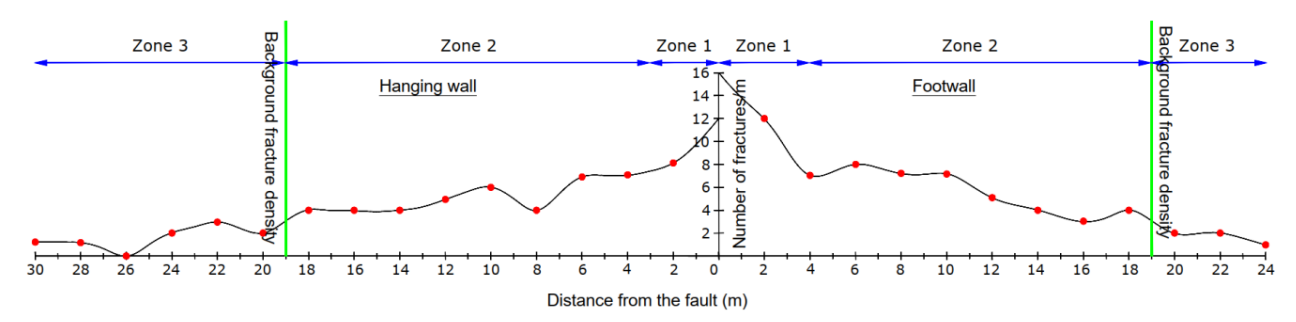


Fig. 14. Fracture density graph measured along the damage zone of (DZ 09) fault zone.

The observed half widths of the fault damage zone (**Figs. 15** and **16**) range between 21m to 32m in the footwall blocks within the Observatory Formation and 18m to 25m in the hanging wall blocks within El-Qurn Formation. This slight variation between the hanging wall and footwall widths may be attributed to differences in the rock unit's properties on either side of the fault, which suggests a notable influence of lithology on the extent of the fault damage zone.

Although the fault displacements differ among the mapped faults, the average half width of the damage zones approached a constant value of 25m, (Fig. 17). The similarity in the measured widths of fault damage zones and fracture distribution at the studied fault damage zones can be attributed to similarity in the deformed carbonate rocks, stress regime, homogenous strain, depth level in Earth's crust, and tectonic events. Consistency in deformed carbonate rocks lying at a certain level in the Earth's crust can be deformed homogenously by the same stress regime.

6. Structural Analysis and Interpretation6.1 En Echelon Fault Belts

One of the prominent structural characteristics of the Cairo-Suez District, including the study area, is the existence of E-W elongated belts of en echelon normal faults (**Fig. 18**). The faults forming each of these belts are characterized also by its left-stepped arrangement. One of these fault belts extend in the study area, which is Maadi El-Qattamiya belt that starts from east Maadi area into the northern scarp of El-Qattamiya Plateau. This belt, like the other fault belts, is characterized by a series of en echelon

faults that dissect the Eocene rocks mainly. The faults within this belt are predominantly oriented in E-W orientation, with some short NW oriented faults.

These E-W elongated en echelon fault belts were interpreted to overlie deep-seated shear zone that were reactivated by dextral strike-slip movement, (Moustafa et al., 1985; and Moustafa and Abd-Allah 1991, 1992). Riedel (1929) and Wilcox et al. (1973) made sandbox and clay cake experiments, respectively to model the structures formed under a deep shear couple. Right-lateral strike-slip movement on a deep-seated fault generates a belt of left-stepping en echelon normal faults, and vice versa (Smith, 1965 and Webster, 1980). These surface faults coalesce at depth into the deep-seated reactivated fault plane (Segall and Polard, 1980).

Accordingly, the left-stepping en echelon normal faults observed in the northern scarp of G. El-Qattamiya and G. Abu Treifiya belt were formed due to dextral strike-slip movements on an underlying deep-seated E-W shear zone.

6.2 Normal Fault Relay Ramps

Several relay ramps have been identified between the overlapping ends of en echelon normal faults, having similar dip directions. The rocks in the relay ramps show a local change in their dip angle and dip direction. Two distinct fault relay ramps have been mapped in the northeastern part of the study area at the northern side of Gebel Abu Treifiya (Figs. 19 and 20). The rocks in these two relay ramps dip toward NW, with a magnitude up to 20°.

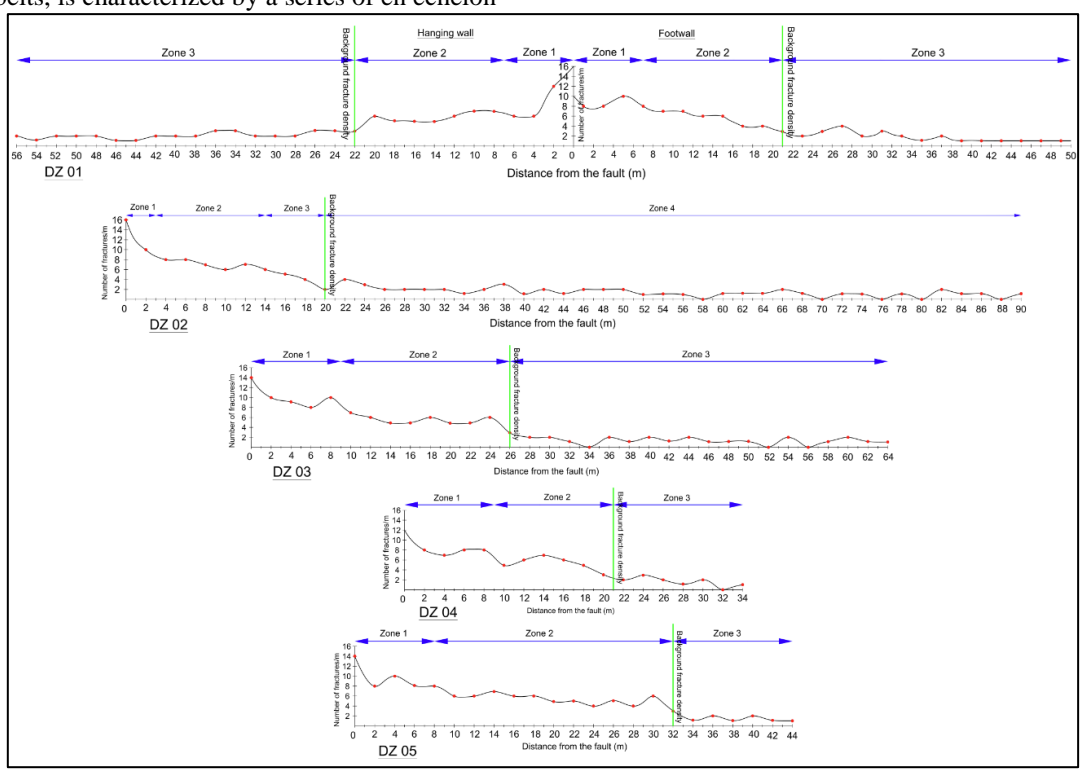


Fig. 15. Fracture density graphs along the damage zones of DZ 01 to DZ 05.

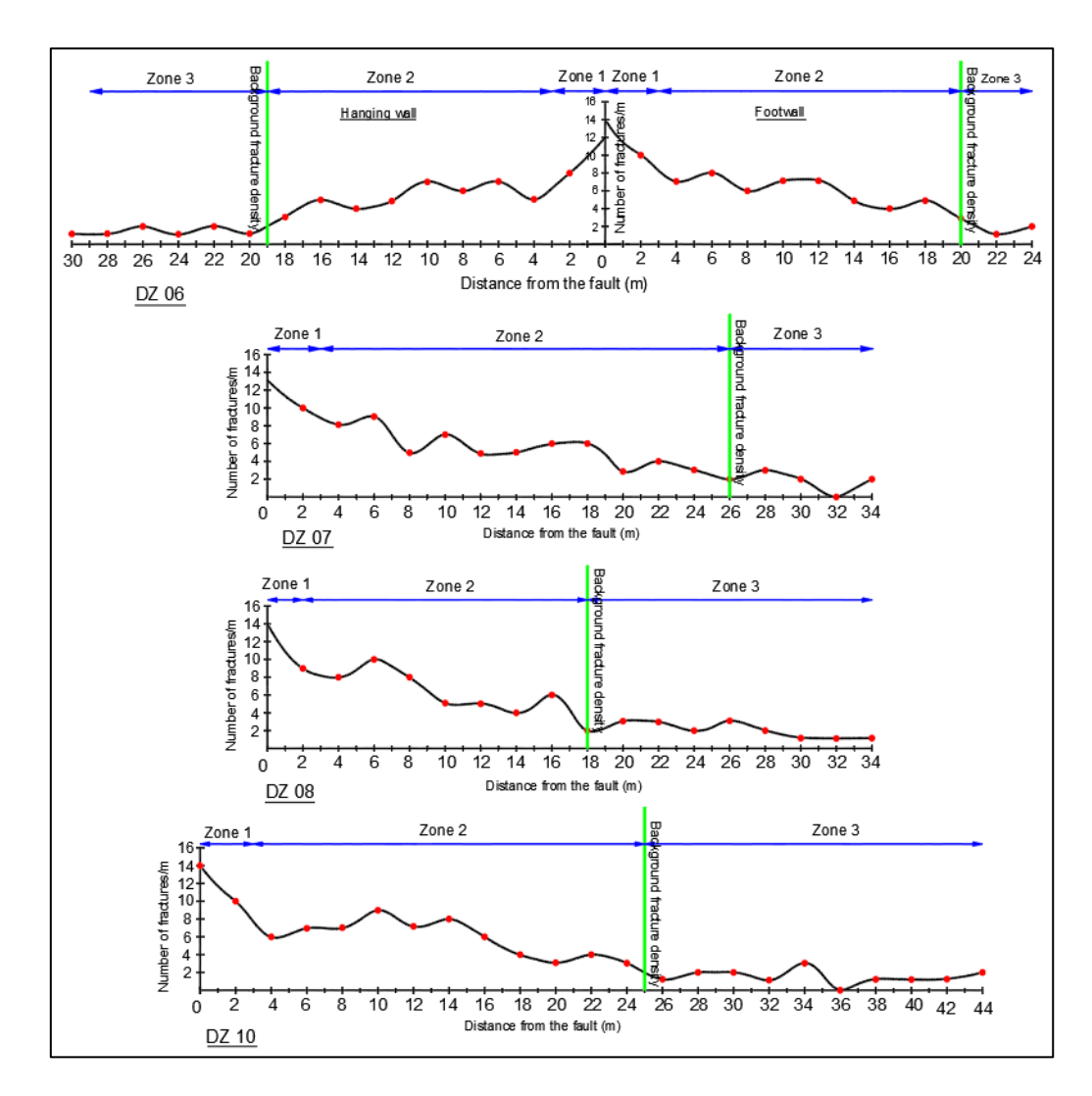


Fig. 16. Fracture density graphs along the damage zones of DZ 06 to DZ 10 (except DZ 09).

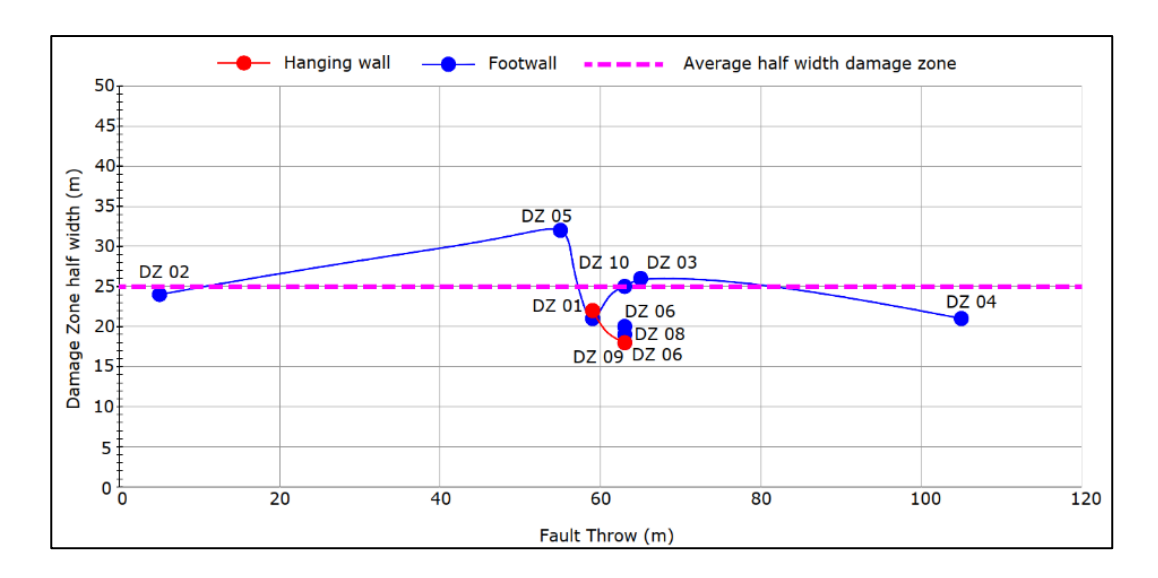


Fig. 17. Graph showing the relationship between the half width of the damage zones and the fault displacement amounts, in addition to the average half width of damage zones.

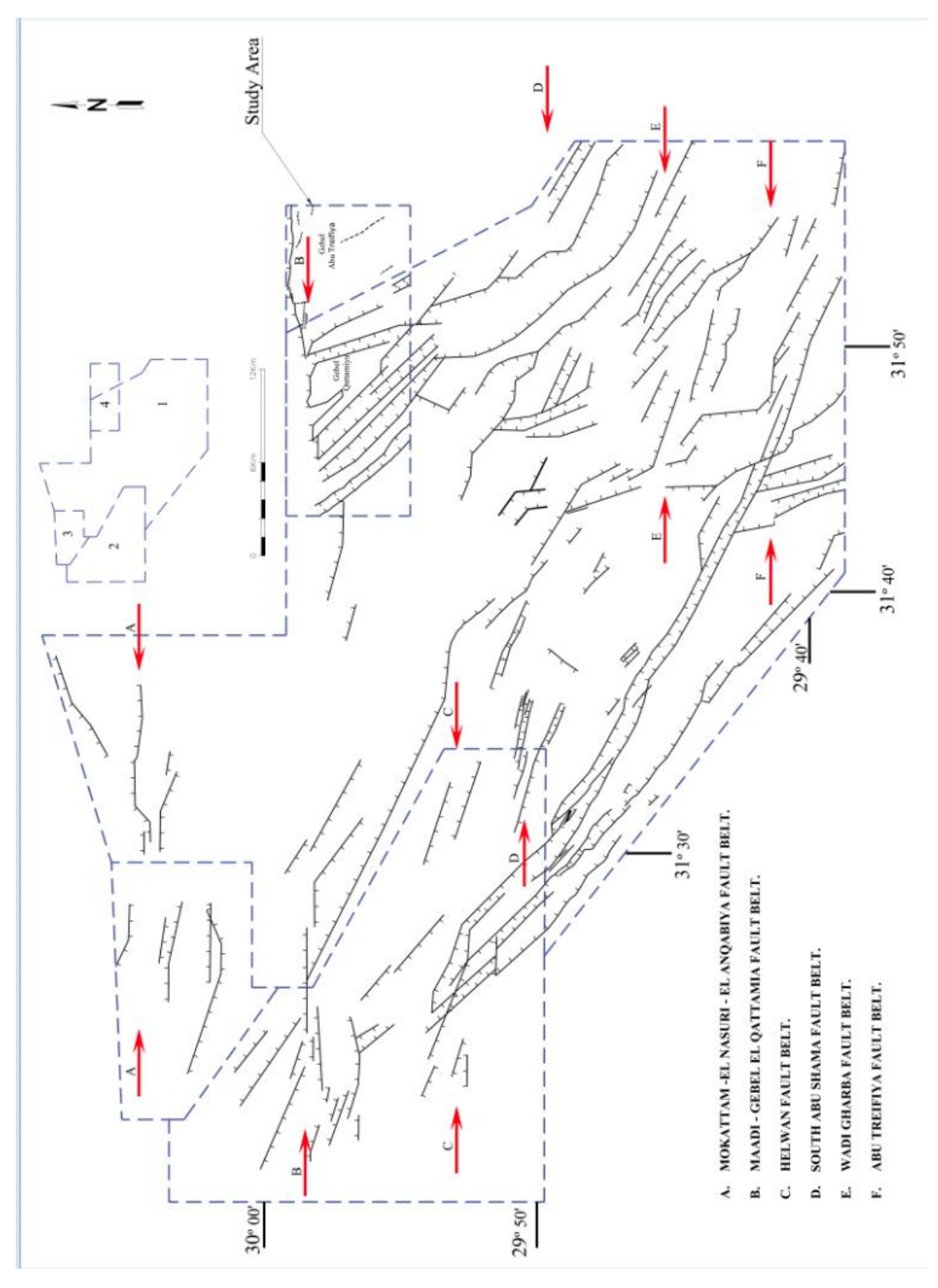


Fig. 18. Faults of the western and central parts of the Cairo-Suez District compiled from Moustafa and Abd-Allah, 1991 (Area 1), Moustafa et al., 1985 (Area 2), and Shukri, 1953 (Area 3), in addition to those of the present study (Area 4). Red arrows indicate six E-W oriented en echelon fault belts.



Fig. 19. Satellite image showing relay ramps (FRR-1 and FRR-2) between two en echelon E-W oriented normal faults bounding the northern side of Gebel Abu Treifiya.



Fig. 20. Field photograph showing relay ramp FRR-2 lying between two en echelon E-W normal faults bounding the northern side of Gebel Abu Treifiya (see Figure 19 for location).

7. Time of Structural Deformation

The mapped faults of the study area dissect the Middle and Upper Eocene rocks indicating that the time of faulting occurred post-Eocene. On the other hand, the Oligocene sediments of Gebel Ahmar Formation as well as the basaltic rocks are confined mainly to the structurally low, down-faulted areas. These stratigraphic and structural settings may indicate that the structural deformation took place during the Late Eocene; before deposition of the Oligocene sediments which were deposited in structurally low areas (grabens). Another alternative

is that the deformation took place after deposition of the Oligocene sediments, but these sediments were eroded from the structurally high blocks later. Field work also indicates the occurrence of silicification and iron-staining of the Oligocene sands and gravels of Gebel Ahmar Formation. This is attributed to the rise of hydrothermal solutions associated with the basaltic extrusion in the area, which indicates that faulting took place before or contemporaneous with the volcanic activity of the Tawab (1986) also reported Abdel silicification of the fault zones in the eastern Greater Cairo region which was taken by him as evidence for faulting before extrusion of the basalts and their associated hydrothermal solutions. The age of basaltic activity of the Cairo-Suez and the Gulf of Suez rift is centered around 23 Ma (whole rock 40Ar/39Ar dates) (Bosworth et al., 2015 and Bosworth and Stockli, 2016). Therefore, we assume that the faults were already present before the 23 Ma basaltic activity.

Gamal et al. (2021) proposed two phases of faulting in the Cairo-Suez region at Gebel Akheider. These are Late Eocene and Oligo-Miocene faulting phases. Their evidence for the late Eocene deformation is the deposition of the Oligocene clastics unconformably above the Middle Eocene rocks in the footwall of a NW-SE oriented normal fault and above the Upper Eocene rocks in the hanging wall block. On the other hand, they attributed the Oligo-Miocene faulting phase to

regional extension associated with the opening of the Gulf of Suez rift and accompanied by the formation of the 23 Ma basaltic rocks. The NW-SE oriented faults related to this Oligo-Miocene faulting phase dissect the Oligocene rocks as well. Accordingly, the time of deformation in the study area is pre-dated the extrusion of the basaltic rocks (i.e. Late Eocene) and were rejuvenated later during the Early Miocene associated with the deformation in the Gulf of Suez rift.

8. Summary and Conclusions

The study area is located to the east of the Greater Cairo region, between the Cairo-Suez Road and the Cairo-Ain Soukhna Road. It is also bordered to the northwest by the New Administrative Capital City. The exposed sedimentary rocks range in age from the Middle Eocene to the Oligocene. A limited extrusive basaltic exposure also exists in the area. The structures affecting the area are mainly normal faults that belong to three predominant sets which are oriented NNW-SSE, NW-SE and E-W. Fault plane striations indicate that these faults have mainly normal and only two faults have diagonalslip with both normal dip-slip and sinistral strikeslip components. The arrangement of normal faults in the study area has resulted in the formation of prominent structural features, such as horsts and grabens, as well as relay ramps. The NNW-SSE fault set comprises 32% of the mapped faults and have high dip angles ranging from 60° to 70°. Their displacements range from less than 25m to 120m and their lengths range between more than 5 km and less than 1 km. The NW-SE oriented fault set comprises 35% of the mapped faults and have dip angles ranging from 60° to 80°. They have mainly normal dip-slip displacement. Their displacements range from less than 50m to 105m and most of them have lengths less than 5 km. The E-W oriented fault set comprises 18% of the mapped faults. They show normal dip-slip displacement, and their dip angles range from 62° to 80°. They have relatively moderate displacements ranging from less than 15m to 90m and have lengths less than 2 km.

Some of the E-W and NW-SE-trending faults have left-stepped en echelon arrangement, forming one E-W elongated belt with relay ramps lying between their overlapping ends. The deformation of the area took place in the Late Eocene and was rejuvenated during the Early Miocene.

The observed differences in the density of faulting between the eastern and western parts of the study area could be related to (i) strain shadow if the thickness and mechanical homogeneity of the sedimentary cover are the same between the two areas and (ii) the presence of more Precambrian faults affecting the high-density faulting

The damage zones of six faults were studied. The observed half width of the fault damage zones ranges between 21m to 32m in footwall blocks within the Observatory and 18m to 25m in the hanging blocks within El-Qurn Formation. This slightly observed variation in the width of the damage zone suggests a significant influence of lithology on the extent of the fault-related damage zone. Furthermore, the field data shows no obvious correlation between fault displacement and the halfwidth of the associated damage zone in either the hanging wall or footwall blocks indicating that the damage zone width is not dependent on the fault displacement. Fracture orientation analysis along damage zones revealed existence of one dominant fracture set trending subparallel to the fault in the footwall and hanging wall, and less dominant set is trending in E-W direction, within the hanging wall. The similarity in the widths of fault damage zones and fracture characteristics can be attributed to similarity in fault-damaged carbonate rocks, stress regime, homogenous strain, depth level in Earth's crust, and tectonic events. Consistency of deformed carbonate that lying at a certain level in the Earth` crust can be deformed homogenously by the same stress regime.

9. References

Abd Allah, A. M. (1988). Structural setting of the area west and southwest of Gebel Qattamia. M.Sc. Thesis, Geol. Dept., Fac. Sci., Ain Shams Univ., Cairo, Egypt, p 117.

Abdel Tawab, S. (1986). Structural analysis of the area around Gebel El Mokattam. M.Sc. Thesis, Geol. Dep., Fac. Sci., Ain Shams Univ., Cairo, Egypt, p 121.

Awad, G. H., Faris, M. I., and *Abbas, H. L.* (1953). Contribution to the stratigraphy of the Mokattam area east of Cairo. *Bulletin de l'Institute du Desert d'Egypte*, 3(2), 106-107.

Bosworth, W., Stockli, D. F., and Helgeson, D. E. (2015). Integrated outcrop, 3D seismic, and geochronologic interpretation of Red Sea dike-related deformation in the Western Desert, Egypt-the role of the 23 Ma Cairo "mini-plume". *J. Afr. Earth Sci.*, 109, 107-119.

- Bosworth, W., & Stockli, D. F. (2016). Early magmatism in the greater Red Sea rift: timing and significance. *Can. J. Earth Sci*, 53(11), 1158-1176.
- Egyptian Geological Survey and Mining Authority (1983). Geologic map of the Greater Cairo area, scale 1:100,000.
- Farag, I. A. M., and Ismail, M. M. (1955). On structure of Wadi Hof area north-east of Helwan. *Bull. Inst. Desert Egypt*, 1(5), 179-192.
- Farag, I. M., & Ismail, M. M. (1959). A contribution to the structure of the area east of Helwan. *Egypt J Geol*, 3, 71-86.
- Gamal, N., Yousef, M., Moustafa, A. R., and Bosworth, W. (2021). Spatiotemporal evolution of transfer structures and linked fault systems in an extensional setting Southwest Gebel Akheider, Cairo-Suez District, Egypt. Mar. Pet. Geol., 133, 105260.
- Ghobrial, G. A. (1971). Geological Studies in the Area East of Maadi, United Arab Republic. M. Sc. Thesis Fac. Sci., Cairo Univ. Egypt, p 114.
- Henaish, A., and Kharbish, S. (2020). Linkage style of rift-associated fault arrays: insights from central Cairo-Suez district, Egypt. CJEES, 15(1), 189-196.
- Henaish, A. (2023). New insights from conjugate transfer zones in the southern Cairo-Suez province: Implications for deformation history and mechanism. *Mar. Pet. Geol.*, 158, 106533.
- Maqbool, A., Moustafa, A. R., Dowidar, H., and Yousef, M. (2014). Structural setting of Gebel Ataqa area, Gulf of Suez, Egypt Implications for rift-related fault array. Eg. J. Geol., 58, 205-221.
- Maqbool, A.R., Moustafa, A.R., Dowidar, H., Yousef, M. (2016). Architecture of fault damage zones of normal faults, Gebel Ataqa area, Gulf of Suez rift, Egypt. *Mar. Pet. Geol.*, 77, 43-53.
- Meneisy, M.Y. (1990). Vulcanicity, in: Said, R. (ed.), *The Geology of Egypt*. A.A. Balkema, Rotterdam, 157-172.
- Moustafa, A. R. (2002). Controls on the geometry of transfer zones in the Suez rift and northwest Red Sea: Implications for the structural geometry of rift systems. *AAPG bulletin*, 86(6), 979-1002.
- Moustafa, A.R., and Abd-Allah, A.M. (1991). Structural setting of the central part of the Cairo Suez District. *Journal of Middle East Research Center, Ain Shams University, Cairo, Egypt*, 5, 133-145.
- Moustafa, A.R., and Abd-Allah A.M., (1992). Transfer zones with en echelon faulting at the northern end of the Suez rift: *Tectonics*, 11(3), 499–506.
- Moustafa, A. R., Yehia, M. A., and Abdel Tawab, S. (1985). Structural setting of the area east of Cairo, Maadi, and Helwan. Middle East Res. Centre, Ain Shams Univ., Sci. Res. Series, 5, 40-64.

- Riedel, W. (1929). Zur Mechanik Geologischer Brucherscheinungen. Zentral-blatt fur Mineralogie. Geologie und paleontologie B, 354-368.
- Saleh, S., Moustafa, A. R., and Pohánka, V. (2021). Impact of inherited structures on present-day tectonics of the northern Red Sea and its western onshore area in Egypt: evidence from 3D gravity inversion and seismicity. Arab. J. Geosci., 14(13), 1250.
- Said, R. (1962). The Geology of Egypt: Amsterdam, *Elsevier Pub. Co.*, 377 p.
- Said, R., (1990). The Geology of Egypt: R. Said, ed., A. A. Balkema, Rotterdam, 45–50.
- Shukri, N.M. (1953). The geology of the desert east of Cairo, *Bull. Inst. Ddsert*, 105, Egypte 312: 89.
- Shukri, N. M., and Akmal, M. G. (1953). The geology of Gebel el-Nasuri and Gebel el-Anqabiya district. *Bull. Soc. Geogr. Egypte*, 26, 243-276.
- Shukri, N. M., and El Ayouty, M. K. (1956). The geology of Gebel Iweibid-Gafra area, Cairo-Suez district. *Bull. Soc. Geogr. Egypt*, 29, 67-109.
- Segall, P., & Pollard, D. D. (1980). Mechanics of discontinuous faults. Journal of Geophysical Research. *Solid Earth*, 85(B8), 4337-4350.
- Smith, J. G. (1965). Fundamental transcurrent faulting in northern Rocky Mountains. *AAPG Bulletin*, 49(9), 1398-1409.
- Strougo, A. (1985a). Eocene stratigraphy of the eastern greater Cairo (Gebel Mokattam-Helwan) area. *Middle East Research Center, Ain Shams University, Science Research Series*, 5, 1-39.
- Strougo, A. (1985b). Eocene stratigraphy of the Giza Pyramids plateau. *Middle East Research Center, Ain Shams University, Earth Science Series*, 5, 79-99.
- Strougo, A., and Abd-Allah, A. M. (1990). Mokattamian stratigraphy of north central Eastern desert (south of maadi-Qattamiya road). *Middle East Research Center, Ain Shams University, Earth Science Series*, 4, 152-175.
- Webster, R. E. (1980). Structural Analysis of Devils River Uplift-Southern Val Verde Basin, Southwest Texas. *AAPG Bulletin*, 64(2), 221-241.
- Wilcox R., Harding T.P., and Seely D.R. (1973). Basic Wrench Tectonics. Am. Assoc. Pet. Geol. Bull., v. 57(1), 74-96.
- Youssef, M. I. (1968). Structural pattern of Egypt and its interpretation. *AAPG Bulletin*, 52(4), 601-614.

الوضع التركيبي للمنطقة الواقعة جنوب العاصمة الإدارية الجديدة، منطقة القاهرة – السويس، مصر

أحمد ناجي '، وحيد هاشم '*، وعبدالصمد خفاجي "، وعادل رمضان مصطفى '

أشركة دبليو اس بي للاستشارات الهندسية، الرياض، المملكة العربية السعودية

تسم الجيولوجيا، كلية العلوم، جامعة عين شمس، القاهرة ، مصر

"قسم العلوم البيولوجية والجيولوجية، كلية التربية، جامعة عين شمس، القاهرة ، مصر

تقع منطقة الدراسة شرق منطقة القاهرة الكبرى، بين طريق القاهرة-السويس وطريق القاهرة-العين السخنة ويحد المنطقة من الناحية الشمالية الغربية المرحلة الأولى من العاصمة الإدارية الجديدة. يهدف البحث إلى دراسة التراكيب الجيولوجية بالمنطقة وتفسير تاريخ تشوهها. وقد تم رسم خريطة جيولوجية للمنطقة بمقياس رسم ١:٢٠٠٠٠ والتي أظهرت مكاشف صخور رسوبية تتراوح أعمارها بين الأيوسين الأوسط والأوليجوسين بالإضافة إلى طفوح بازلتية محدودة. يكون هذا التتابع هضبتين وهما هضبة القطامية وهضبة أبوطريفية بينهما منخفض أم ريحيات. تتأثر صخور الإيوسين الأوسط والإيوسين العلوي بثلاث أطقم رئيسية من الصدوع العادية تتخذ اتجاهات شمال شمال غرب، وشمال غرب، وشرق - غرب. تتخذ الصدوع المتجهة شرق - غرب، وبعض الصدوع المتحهة شمال غرب، نسقا سلميا يساري الترتيب ربما نشأ نتيجة حركة تزبح مضرب يمينة أثرت على نطاقات قص عميقة كامنة تحتها. أما الصدوع المتجهة شمال شمال غرب والمتجهة شمال غرب فتتميزا بإمتدادهما لمسافة كبيرة مكونة إزاحة رأسية كبيرة نسبيا. وتعمل أحزمة الصدوع المتجهة شرق-غرب كنطاقات نقل بين الصدوع الرئيسية المتجهة شمال غرب وشمال شمال غرب. وقد نشأت هذه التراكيب قبل الطفح البركاني في نهاية عصر الأيوسين المتأخر، وتجدد نشاط هذة التراكيب لاحقا أثناء الميوسين المبكر. تتميز النطاقات التدميرية للصدوع بوجود نفس التشوهات الصخرية تقريبا، حيث إن نطاقات الصدوع المتجهة شمال غرب وشرق - غرب تتميز بثبات عرض هذه النطاقات رغم تغير أطوال وازاحة صدوعها. ويمكن إعزاء هذا العرض شبه الثابت لنطاقات الصدوع إلى التشابه في صخور الكربونات المتأثرة بهذة الصدوع، ونظام الإجهاد، والانفعال المتجانس، ومستوى العمق في قشرة الأرض، والأحداث التكتونية. تشكل الكسور في النطاقات التدميرية داخل نطاقات الصدوع طقمان: طقم الكسور الرئيسي يتخذ اتجاها مواز إلى شبه مواز لاتجاه الصدع الرئيسي، وترتبط نشأته بحقول الإجهاد المحلية المحيطة بالصدع الرئيسي، وطقم الكسور الثاني (الأقل تمثيلًا)، يتخذ اتجاها مائلًا على مضرب الصدع. بينما ترتبط نشأته بحركة تزيح المضرب اليمينية الذي أثرت في نطاقات القص العميقة.